

Early warning of precessing neutron-star black-hole binary mergers with the near-future gravitational-wave detectors

Takuya Tsutsui,^{1,2*} Atsushi Nishizawa,¹ and Soichiro Morisaki³

¹Research Center for the Early Universe (RESCEU), Graduate School of Science, The University of Tokyo, Tokyo 113-0033, Japan

²Department of Physics, Graduate School of Science, The University of Tokyo, Tokyo 113-0033, Japan

³Department of Physics, University of Wisconsin-Milwaukee, Milwaukee, WI 53201, USA

Accepted XXX. Received YYY; in original form ZZZ

ABSTRACT

Since gravitational and electromagnetic waves from a compact binary coalescence carry independent information about the source, the joint observation is important for understanding the physical mechanisms of the emissions. Rapid detection and source localization of a gravitational wave signal are crucial for the joint observation to be successful. For a signal with a high signal-to-noise ratio, it is even possible to detect it before the merger, which is called early warning. In this article, we estimate the performances of the early warning for neutron-star black-hole binaries, considering the precession effect of a binary orbit, with the near-future detectors such as A+, AdV+, KAGRA+, and Voyager. We find that a gravitational wave source can be localized in 100 deg^2 on the sky before $\sim 10\text{--}40$ s of time to merger once per year.

Key words: gravitational waves – radiation mechanisms:general – methods: observational – (stars:) gamma-ray burst: general – stars: neutron

1 INTRODUCTION

In 2017, two advanced LIGO (aLIGO) detectors (Aasi et al. 2015; Harry 2010) and advanced Virgo (AdV) (Acernese et al. 2015) detected a gravitational wave (GW) from a coalescence of binary neutron stars (BNS) (Abbott et al. 2017b), dubbed as GW170817. This event was followed up by many electromagnetic (EM) telescopes in broad bands and provided much information on an EM counterpart (Abbott et al. 2017c). From the successful joint observation by GWs and EM waves, the association of a short gamma-ray burst (sGRB) with a merger of BNS was confirmed. Furthermore, there are many benefits for not only sGRB but also the identification of the host galaxy, observations of kilonova (Metzger 2019), measurement of Hubble constant (Schutz 1986) and so on. It is desirable to increase the successful probability of the EM follow-up.

Rapid detection and source localization of a GW signal are crucial for the joint observation to be successful. Then, one of the ways to improve the successful probability is early warning forecasting where and when a binary merger happens (Cannon et al. 2012; Sachdev et al. 2020; Magee et al. 2021). With the alert, one can wait for the merger with EM telescopes pointed there. Then we could observe prompt emission from a BNS merger (Nakar 2007), resonant shattering (Tsang et al. 2012), tidal disruption in neutron-star black-hole (NSBH) binaries (McWilliams & Levin 2011), and so on.

Now there are two aLIGO detectors, AdV, and KAGRA (Somiya 2012), called second-generation (2G) detectors. The 2G detectors can detect GWs but not localize the sources before the merger well (Magee et al. 2021). Those detectors are planned to be upgraded to A+s (Abbott et al. 2016), AdV+ (Degallaix (the Virgo Collabora-

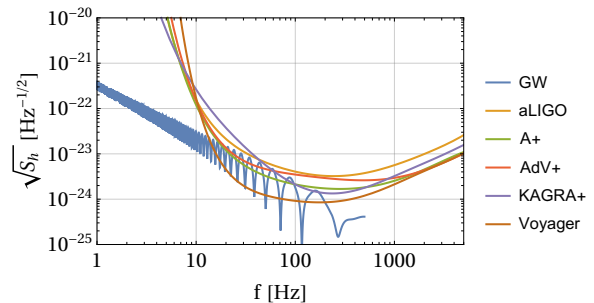


Figure 1. Typical GW spectrum from a precessing NSBH merger at $z = 0.05$ (blue) and power spectral densities for aLIGO (orange), A+ (green), AdV+ (red), KAGRA+ (purple) and Voyager (brown) (Aasi et al. 2015; Abbott et al. 2016; Degallaix (the Virgo Collaboration) 2018; Michimura et al. 2020; Adhikari et al. 2020).

tion) 2018) and KAGRA+ (Michimura et al. 2020) from the O5 observing run starting later than 2025. Furthermore, Voyager (Adhikari et al. 2020) is also planned the construction after 2030. These GW detectors are called 2.5G detectors in this article. They are more sensitive than the current detectors (Fig. 1) so that the early warning by them provides longer time to merger. The early warning of BNS with the 2.5G detectors has been studied (Nitz et al. 2020; Magee & Borhanian 2022). Since the early warning is in the spotlight recently, there are many similar works: early detection with 2G detectors by neural networks (Yu et al. 2021; Baltus et al. 2021; Wei & Huerta 2021), estimations of the performances of early warning with third generation (3G) detectors (Chan et al. 2018; Tsutsui et al. 2021; Nitz & Canton 2021) such as Einstein Telescope (Punturo et al. 2010) and Cosmic Explorer (Abbott et al. 2017a), early warning by consider-

* E-mail: tsutsui@resceu.s.u-tokyo.ac.jp

ing higher modes of a GW (Kapadia et al. 2020; Singh et al. 2021). Recently, NSBH and NSBH-like mergers have been detected (Abbott et al. 2020, 2021b,a), but their EM counterparts have not been reported yet. Since the physics of the EM counterparts of the BNS and NSBH mergers could be different, we should consider the both possibilities as the targets of the early warning.

In this article, we consider the performance for NSBH binaries. For such asymmetric binaries, a precession effect can be important if either or both of compact objects have non-zero misaligned spins. Since the total angular momentum of a binary is not parallel with the orbital angular momentum, the orbital plane precesses and the amplitude of a GW from the binary is modulated (Apostolatos et al. 1994; Lundgren & O’Shaughnessy 2014; Brown et al. 2012). By increasing information about the binary in the waveform, the estimation precision of binary parameters should be improved.

The organization of this article is as follows. In Sec. 2, we review waveforms from precessing binaries and the Fisher analysis to estimate the performance of early warning to the waveforms. We show in Sec. 3 the parameter estimation errors as a function of frequency or time to merger for different networks of detectors and discuss the results in Sec. 4, compared with the current EM observations and previous studies on the early warning. Sec. 5 is devoted to a summary.

2 ANALYSIS

Non-precessing binaries are frequently considered as GW sources for simplicity. However, in reality, BHs may have non-zero spins. Then a precessing spin induces the amplitude modulation of a GW and help improve the sky localization of a source. We review the GW waveform from a precessing binary in Sec. 2.1. The precession effect is strong for high mass-ratio binaries, and then we consider NSBH binaries. In Sec. 2.2, we estimate the number of NSBH binaries that we observe in a year and identify the highest-signal-to-noise-ratio (SNR) event in the realistic period of observations. After that, we briefly explain the settings for estimating the performance of early warning with the Fisher matrix in Sec. 2.3.

2.1 Waveform

An analysis in this article to estimate early warning performances is basically same as in (Tsutsui et al. 2021). Thus, we briefly review the waveform in this subsection. The readers can refer to (Tsutsui et al. 2021) for the details.

For ease to read this article, we summarize the independent arguments set for the waveform:

$$\{\lambda_i\} = \{\mathcal{M}, \eta, \chi, t_c, \phi_c, d_L, \theta, \phi, \psi, \theta_J, \kappa, \alpha_0\}, \quad (1)$$

\mathcal{M} is the chirp mass, η is the symmetric mass ratio, χ is the dimensionless spin magnitude of a heavier component (BH), t_c is the coalescence time, ϕ_c is the coalescence phase, d_L is the luminosity distance, θ and ϕ are the longitude and latitude of GW source, ψ is the polarization angle, θ_J is the inclination angle of total angular momentum, κ is a inner product of unit vectors of the orbital and spin angular momentum and α_0 is the initial precession angle. We note that the spin magnitude of a lighter component (NS) is neglected here because it is much smaller than χ for NSBH binaries. Also, the orbital eccentricity is not considered.

The GW waveform from a precessing compact binary is a product of the amplitude factor and the phase factor for non-precessing case and antenna response factor including the precession effect (see Fig. 1

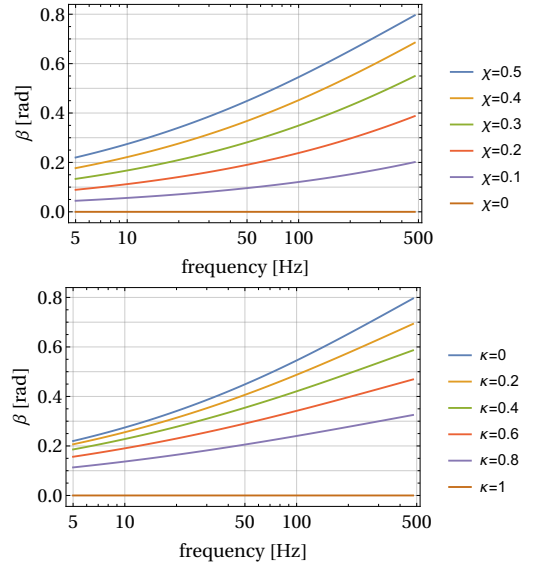


Figure 2. Precession angle β as a function of frequency from f_{\min} to f_{isco} for some χ (left) and κ (right).

for the typical spectrum of a GW from the precessing binary):

$$\tilde{h}_I(f) = Z_I(f) A(f) e^{2i(\Phi_{\text{orb}} - \zeta) + \phi_{I, \text{Doppler}}}, \quad (2)$$

$$A(f) = \left(\frac{5\pi}{24}\right)^{1/2} \frac{G^2 \mathcal{M}^2}{c^5 d_L} \left(\frac{\pi G M f}{c^3}\right)^{-7/6}, \quad (3)$$

$$Z_I(f) = (C_+(\alpha, \beta, \zeta) F_{I,+} + C_\times(\alpha, \beta, \zeta) F_{I,\times}) - i (S_+(\alpha, \beta, \zeta) F_{I,+} + S_\times(\alpha, \beta, \zeta) F_{I,\times}) \quad (4)$$

The phase factor includes the orbital phase up to 1.5PN from (Will & Wiseman 1996; Tsutsui et al. 2021; Husa et al. 2016; Khan et al. 2016), and the Doppler phase between the I -th detector at \vec{r}_I and the geocenter, $\phi_{I, \text{Doppler}} = -2\pi i f \vec{r}_I \cdot \vec{n}/c$. The antenna response factor is written by mixtures of the antenna responses for non-precessing one, $F_{I,+/\times}$, with coefficients originated from precession effect, $C_{+/\times}$ and $S_{+/\times}$ (Tsutsui et al. 2021; Lundgren & O’Shaughnessy 2014; Brown et al. 2012; Apostolatos et al. 1994). Although there are three parameters (α, β, ζ) to express the precession effect, the one parameter is defined here because the other parameters are less important to estimate the performance of early warning (Tsutsui et al. 2021):

$$\beta(v) = \cos^{-1} \left[\frac{1 + \kappa \gamma}{\Gamma_J} \right], \quad (5)$$

where

$$\gamma(v) = \frac{|\vec{S}|}{|\vec{L}|} = \frac{m_1 \chi}{m_2} v, \quad (6)$$

$$\Gamma_J(v) = \frac{|\vec{J}|}{|\vec{L}|} = \sqrt{1 + 2\kappa \gamma + \gamma^2}, \quad (7)$$

$$\kappa = \frac{\vec{L}}{|\vec{L}|} \cdot \frac{\vec{S}}{|\vec{S}|}, \quad (8)$$

v is the velocity of the component masses from Kepler law. The frequency dependences of the β for some parameters are in Fig. 2. Since $\chi = 0$ or $\kappa = 1$ case means non-precessing, β s are always zero. We choose 0.5 as our fiducial value of χ for our simulated NSBHs. This value is consistent with the estimated primary spin of GW200115 (Abbott et al. 2021b).

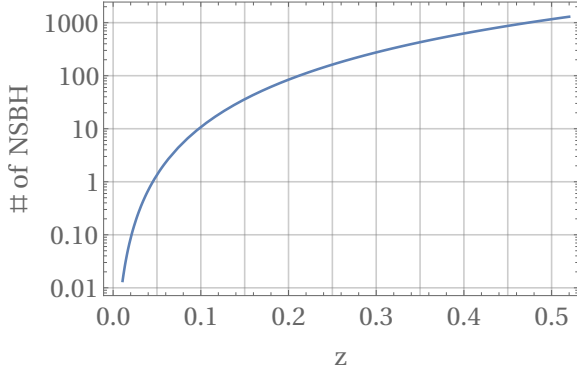


Figure 3. The cumulative number of NSBH mergers per year as a function of redshift z .

Table 1. z_{\max} and the average number of NSBH mergers per year for the different detector networks. V+ means AdV+ and K+ means KAGRA+.

network	z_{\max}	the average number of NSBH mergers [1/yr]
A+A+V+	0.185	66.9
A+A+V+K+	0.212	99.9
3 Voyagers	0.517	1274

2.2 Event rate

The number of sources available for the measurement of GW N is estimated here as a function of redshift z . The number of sources between redshifts z and $z + dz$ is given by, e. g. (Nishizawa 2016),

$$\frac{dN}{dz} = \frac{4\pi cr(z)^2 \dot{n}(z) T_{\text{obs}}}{(1+z)H(z)} \quad (9)$$

where T_{obs} is the observation time, $\dot{n}(z)$ is the merger rate per unit comoving volume and unit proper time at redshift z , $r(z)$ is the comoving distance and $H(z)$ is the Hubble parameter. For the merger rate at $z < 1$, we take a linear evolution,

$$\dot{n}(z) = \dot{n}(0)(1 + 2z), \quad (10)$$

which is based on the observation of the star formation history and is used in (Nishizawa 2016). For NSBH binaries, we assume $\dot{n}(0) = 30 \text{ Gpc}^{-3} \text{ yr}^{-1}$ (Abadie et al. 2010)¹. The integration of (9) is shown in Fig. 3. A NSBH merger happens 1 per year at $z = 0.05$. For comparison, we show z_{\max} at which SNR = 8 and the number of NSBH mergers for the detector networks in Table 1.

2.3 Fisher analysis

To estimate the parameter errors, we use the Fisher information matrix, F_{ij} , defined between $f_{\min} = 5 \text{ Hz}$ and the innermost stable circular orbit frequency for a Schwarzschild BH, $f_{\text{ISCO}} = \frac{1}{12\sqrt{6}\pi} \frac{c^3}{G(m_1+m_2)}$:

$$F_{ij}(f) = 4\Re \int_{f_{\min}}^f \frac{\partial_i \tilde{h}^*(f') \partial_j \tilde{h}(f')}{S_n(f')} df' + \frac{\delta_{ij}}{(\delta\lambda_i)^2}, \quad (11)$$

¹ Recently the merger rate from the observation of NSBH binaries was reported as $\dot{n}(0) = 45^{+75}_{-33} \text{ Gpc}^{-3} \text{ yr}^{-1}$ (Abbott et al. 2021b) when we were preparing the draft. Here we use the previous rate estimated from the population synthesis simulations, but our results hardly change if we take the median rate.

Table 2. Medians of time-to-merger for NSBH binaries when the conditions for the network SNR, $\Delta\Omega$, and ΔN are satisfied. The values in this table are in the unit of seconds. “w/o” and “w/” mean “without” and “with” the precession effect, respectively.

network	time to merger [s]					
	A+A+V+		A+A+V+K+		3 Voyager	
precession	w/o	w/	w/o	w/	w/o	w/
network SNR= 8	24	24	25	25	64	64
$\Delta\Omega = 300 \text{ deg}^2$	13	23	19	25	35	57
$\Delta\Omega = 100 \text{ deg}^2$	4.2	9.6	7.9	12	19	36
$\Delta N = 10^4$	3.7	18	7.2	20	20	50
$\Delta N = 10^3$	0.20	4.1	1.1	5.8	5.5	25
$\Delta N = 10^2$	-	0.22	0.07	0.90	0.49	8.3

where ∂_i is a partial derivative with respect to the parameter λ_i . Although f_{ISCO} ideally depends on χ (Jefremov et al. 2015), the dependence can be neglected because our interest is early warning, that is, the low-frequency region of the Fisher matrix F_{ij} . We have taken into account the prior effects (the second term) as done in (Tsutsui et al. 2021) where $S_n(f)$ is a power spectral density, δ_{ij} is the Kronecker delta, and $\delta\lambda_i$ is a 1σ error of a Gaussian distribution and is taken as a physical range of the parameter. From the Cramer-Rao inequality (Cutler & Flanagan 1994), the inverse Fisher matrix F_{ij}^{-1} can be recognized as the covariance matrix.

In this article, we quantify the performance of early warning by the 1-sigma statistical errors of the luminosity distance, the sky localization error, Δd_L and $\Delta\Omega$, and the number of galaxies in the error volume, ΔN , as functions of time to merger

$$t_c - t = \frac{5}{256} (\pi f)^{-8/3} \left(\frac{GM}{c^3} \right)^{-5/3}, \quad (12)$$

at the Newtonian order (Maggiore 2008; Creighton & Anderson 2011). The Fisher matrix is calculated for 200 samples² with the following choice of fiducial parameters of a spinning BH and a non-spinning NS: the angles, (θ, ϕ) and (θ_J, ψ) , are isotropically sampled. The masses and spins are $\chi = 0.5$, $\kappa = 0$, $m_1 = 7 M_\odot$ and $m_2 = 1.4 M_\odot$. The redshift z is 0.05 from the discussions in Sec. 2.2. In Sec. 3.2, we also consider the performance for other parameters, $\chi = 0.1, 0.2$ and $\kappa = \cos 30^\circ, \cos 45^\circ$, and verify that the estimation errors are not degraded significantly. We consider the 2.5G detectors: A+s, AdV+, KAGRA+, and Voyager at Hanford, Livingston and Virgo sites. They are the upgrades of the current detectors at the same sites. Also, as with (Tsutsui et al. 2021), the Earth rotation effect is taken into account, although the observable duration is much shorter than the previous case and the effect is almost negligible.

3 RESULT

3.1 network dependence

Figure 4 are the medians of the network SNR, the sky localization errors Δd_L and distance errors Δd_L , and the number of galaxies in the error volume ΔN , for the detector networks, (A+, A+, AdV+), (A+, A+, AdV+, KAGRA+), and 3 Voyagers. Since the precession

² The choice of the number of samples is due to computation time. As the precession effect is not simple, we take ~ 2 days for one network and one parameter set with a reasonable computer. So we have to spend $O(\text{a month})$ in total. Since the estimations are from 200 samples, the results provided in this article have $\sim 7\%$ error.

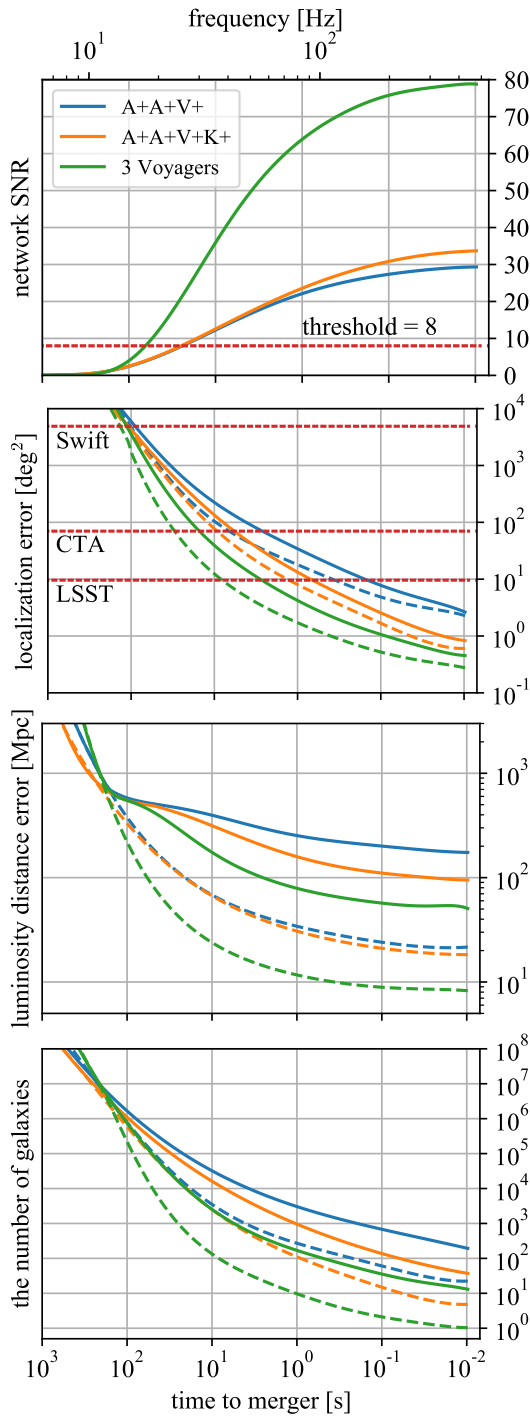


Figure 4. Medians of localization errors with A+s at Hanford and Livingston sites and AdV+ (blue), those plus KAGRA+ (orange), and three Voyagers at Hanford, Livingston, and Virgo sites (green) as a function of time to merger. The panels from the top to the bottom are for the network SNR without the precession effect, the sky localization error, the distance error, and the number of galaxies in the error volume. Solid (dashed) lines are without (with) the precession effect. The red dotted line in the network SNR plot represents the SNR threshold for detection at 8. The red dotted lines in the sky localization plot represent the typical field of views of Swift, CTA, and LSST (4900 deg^2 , 70 deg^2 , and 9.6 deg^2), respectively.

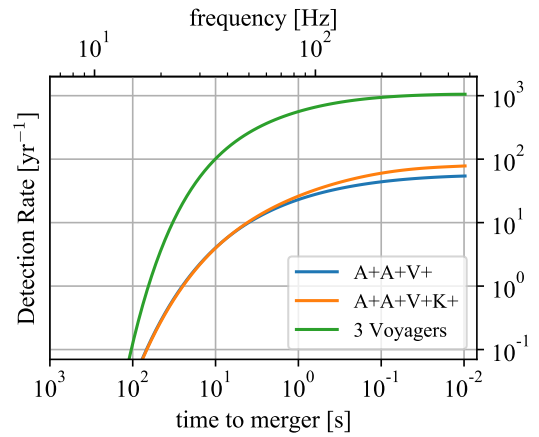


Figure 5. Detection rate for non-precessing binaries with A+s at Hanford and Livingston sites and AdV+ (blue), those plus KAGRA+ (orange), and three Voyagers at Hanford, Livingston, and Virgo sites (green) as a function of time to merger. Explanations for the width of distributions are written in Sec. 3.1

effect affects the variance of SNR but not the median (the measured relative difference is $\lesssim 2\%$), the network SNRs are plotted only for non-precessing cases in Fig. 4. To convert the error volume to the number of galaxies ΔN , the number density of the galaxies is assumed to be 0.01 Mpc^{-3} as explained in more detail in (Nishizawa 2017). The time to mergers when $\Delta\Omega$ and ΔN reach typical values are summarized in Table 2.

GW detection alerts are generated when the network SNR exceeds 8 and can be sent out before the merger at 24 s for two A+s and AdV+, 25 s for two A+s, AdV+ and KAGRA+, and 64 s for three Voyagers. At that times, for a precessing (non-precessing) case, the sky localization errors are 323 deg^2 (625 deg^2), 300 deg^2 (464 deg^2), and 423 deg^2 (1158 deg^2), respectively.

In Fig. 4, the estimations with the precession effect are much improved, especially for Δd_L then ΔN . However, the improvement for $\Delta\Omega$ is relatively smaller because $\Delta\Omega$ has already been well determined by arrival-timing measurements of a GW, and the precession effect does not help much. On the other hand, the degeneracy between the luminosity distance and the inclination angle is broken by precession (Vecchio 2004; Vitale et al. 2014), and then Δd_L is significantly improved.

Figure 5 is the detection rate for the detector networks, that is, the expected number of the GW sources with the SNR higher than the detection threshold 8. As in the plot of network SNR in Fig. 4, the detection rates are for only a non-precessing case. From Fig. 5, we can find how many events are detectable at a time-to-merger, e.g. the GW events with the detection rate 10 yr^{-1} , which corresponds to $z \sim 0.1$ from Fig. 3, can be detected at 3.0 s for A+s and AdV+, 3.7 s for those plus KAGRA+ and 30 s for three Voyagers, before the merger. From the uncertainties of SNRs in 200 samples, the lines in Fig. 5 have the width of distributions (1σ) for the precessing (non-precessing) case; 68% (84%) for A+s and AdV+, 53% (73%) for those plus KAGRA+ and 58% (78%) for three Voyagers.

3.2 parameter dependence

In the previous subsection, we considered our fiducial set of source parameters. However, in reality, mass and spin parameters have the distributions depending on the astrophysical formation channel and are still highly uncertain (Abbott et al. 2021b). To show param-

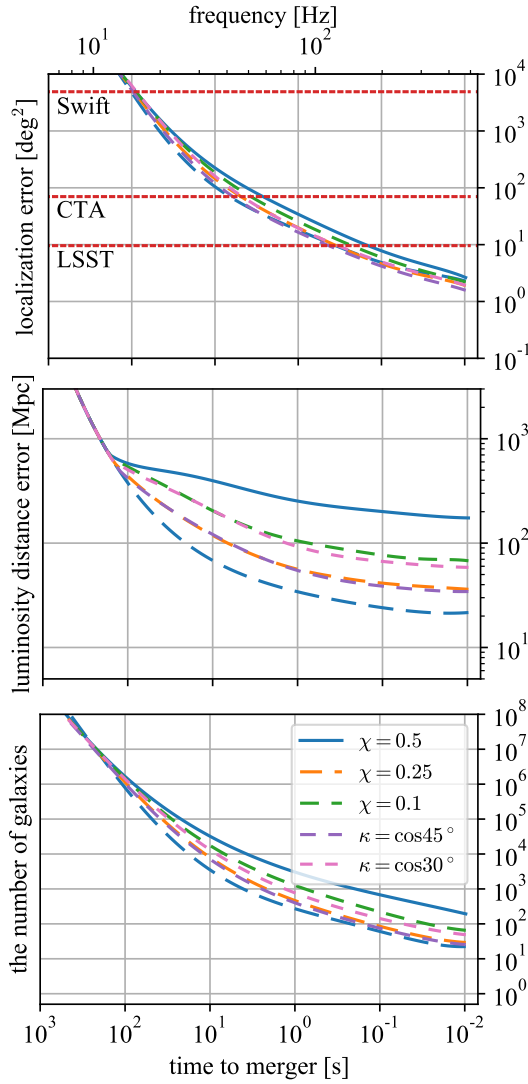


Figure 6. Medians of localization errors with A+s at Hanford and Livingston sites and AdV+ for some parameters. The solid line is for non-precessing case and the dashed lines are for precessing case. The blues are for $(\chi, \kappa) = (0.5, 0)$, the orange for $(0.25, 0)$, the green for $(0.1, 0)$, the purple for $(0.5, \cos 45^\circ)$, pink for $(0.5, \cos 30^\circ)$

ter dependences, we estimate the performances for less-precessing NSBHs with some χ and κ .

χ does not affect the SNR evolutions in our approximated waveform because it does not appear in GW amplitude. Also, κ does not affect the median of the SNR evolution although the variance of SNR is affected (same as Sec. 3.1). Then, the SNR evolutions are same as those in Fig. 4. The estimated performances of $\Delta\Omega$, Δd_L , and ΔN are in Fig. 6 and 7. For simplicity, the performances for non-precessing case except for $\chi = 0.5$ and $\kappa = 0$ are omitted in both figures. In both figures, the improvements of $\Delta\Omega$ are almost same because the maximum improvement in the case of $\chi = 0.5$ is not large, that is, the performances for $\Delta\Omega$ are robust even for less-precessing parameters.

For Δd_L and ΔN , the result for $(\chi, \kappa) = (0.25, \cos 90^\circ)$ and $(0.5, \cos 30^\circ)$ are almost same with that for $(0.5, \cos 45^\circ)$ and $(0.1, \cos 90^\circ)$, respectively. This is because the time evolutions of β for those are almost same between those parameter sets (see Fig. 2). In other word, the improvements for Δd_L and ΔN are proportional

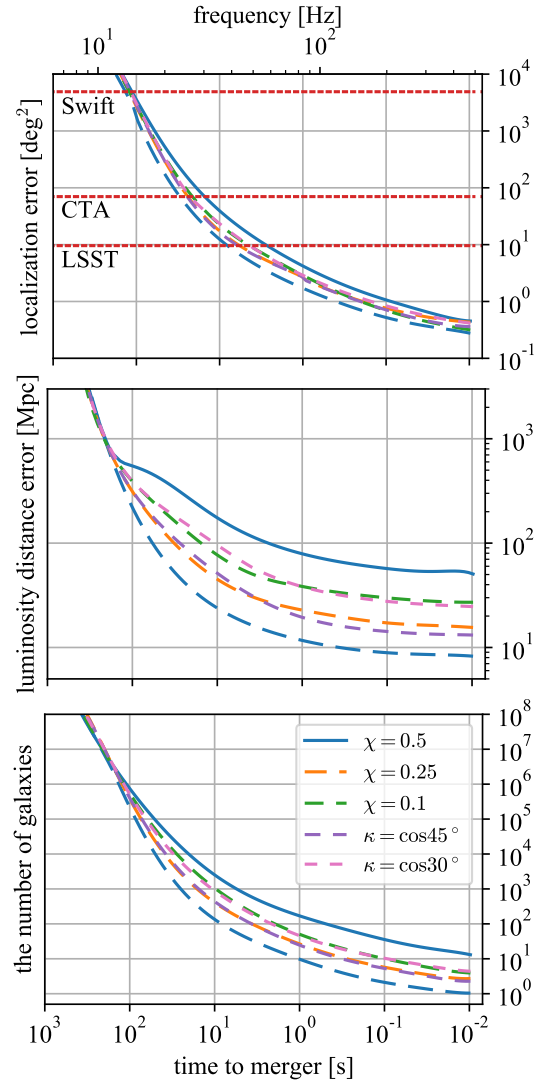


Figure 7. Medians of localization errors with three Voyagers at Hanford, Livingston and Virgo sites for some parameters. The lines and parameters chosen are the same as those in Fig. 6.

to β , so that we can obtain performances for other parameters from Eq. (5).

Also the component masses can be changed. However, the chirp mass is varied by $\sim 30\%$ in the mass range that EM radiation is expected (Foucart et al. 2018). Then the difference of the performances for the range is $\sim 30\%$ (Tsutsui et al. 2021).

4 DISCUSSIONS

4.1 EM telescopes

Here we compare our results of the sky localization with the field of view (FoV) of typical EM telescopes. The FoV is $\sim 70 \text{ deg}^2$ for CTA-SST (Bartos et al. 2018; Acharyya et al. 2019), $\sim 4900 \text{ deg}^2$ for Swift-BAT (Barthelmy et al. 2005), $\sim 2.6 \times 10^4 \text{ deg}^2$ for Fermi-GBM (Digel & Myers 2001), and $\sim 9.6 \text{ deg}^2$ for LSST (Ivezic et al. 2019). Swift and Fermi are all-sky sweeping surveys. CTA can point to the EM counterpart in $\lesssim 1 \text{ min}$. LSST can tilt by 3.5 deg in 5 s and needs $20 \text{ s} - 40 \text{ s}$ for the exposure. From Fig. 4, for the all detector networks, the EM counterpart can be inside the FoV of Swift and

Fermi before ~ 100 s of the merger. On the other hand, it can be inside that of CTA and LSST before $O(0.1 - 1)$ s for a non-precessing case and $O(1 - 10)$ s for a precessing case. Thus, with the early warning for NSBH binary mergers, precursor emissions can be observed before the merger by Swift and Fermi, and prompt emissions and afterglows from sGRB can be observed by CTA and LSST.

So far we have not taken into account latencies produced by the data acquisition of GW detectors and EM telescopes, the detection of a GW signal, and the localization of a GW source. Especially, the parameter inference taking into account the precession effects is computationally costly, and takes around half a day even with a fast method to evaluate likelihood (Smith et al. 2016). The development of a fast localization technique incorporating the precession effect is necessary for early warnings of NSBH events.

4.2 GW Detector networks

In Fig. 4, the results for two A+s and AdV+ are similar to those for two A+s, AdV+, and KAGRA+. However, it does not mean that a fourth detector is unnecessary for multi-messenger observations. The first advantage is duty cycle. The duty cycle that at least three active detectors out of four detectors is much higher than the one that three active detectors out of three detectors, i. e. 51% increases to 82% given a single-detector duty cycle of 80%. The second advantage is multimodality in the sky localization. When three detectors are at work and only the arrival-time differences between detectors are measured, a mirror candidate spot in the sky probability map always appears above/below the plane spanned by the detectors. By adding a fourth detector to the network, a mirror candidate spot can be eliminated. Then EM observers can avoid pointing their telescopes to the fake sky direction. From these two reasons, the fourth detector is important for the multi-messenger astronomy.

4.3 Comparison with previous studies

The similar study on the early warning with the 2.5G detector networks but for BNS has been done in (Nitz et al. 2020). The times of the early warning before merger for $\Delta\Omega = 100 \text{ deg}^2$ are 54 s for two A+s and AdV (not AdV+) and 194 s for three Voyagers. On the other hand, our results for $\Delta\Omega = 100 \text{ deg}^2$ without the precession effect are 4.2 s for two A+s and AdV+ and 19 s for three Voyagers. Their results are much better than ours. The most dominant reason for the difference is the sources considered. We assume NSBH binaries but they assume BNS. Since the chirp mass of the latter is smaller and its frequency evolution is slower, BNS provide a factor of 4 longer time-to-merger than NSBH binaries, as explicitly seen in (12). There are minor differences which can explain another factor of the difference: the source distance, the credible levels of sky localization error, the sensitivity of Voyager, the detector networks. Since an EM counterpart of NSBH mergers is different from that of the BNS merger, we should consider them as targets for the early warning.

For 3G detectors that will start observations from the mid in 2030s, the early warning for NSBH binary coalescences at $z = 0.1$ can be done typically with the times to merger of 12 – 15 minutes and 50 – 300 seconds when the sky localization areas reach 100 deg^2 and 10 deg^2 , respectively (Tsutsui et al. 2021). In addition, not only Δd_L but also $\Delta\Omega$ are significantly improved due to the precessing effect. This is because the sensitive frequency band of the 3G detectors is much broader than that of the 2.5G detectors, particularly at lower frequencies, and allows us to observe NSBH binaries for ~ 8 hours. Then the Earth rotation and precession effects can break parameter degeneracies much more efficiently.

5 CONCLUSION

The combination of GW and EM observations can provide much information about the source. Rapid detection and source localization of a GW signal are crucial for the joint observation to be successful. It can be done by early warning which forecasts where and when a binary merger happens before the merger (Cannon et al. 2012; Sachdev et al. 2020; Magee et al. 2021). We estimate the performances of the early warning for some detector networks from A+s, AdV+, KAGRA+ and Voyager for precessing and non-precessing NSBH binaries. As a result, we found that the direction can be known with $\Delta\Omega = 100 \text{ deg}^2$ in ~ 10 s–40 s before the merger. The improvement by considering the precession effect is about a factor ~ 2 for the sky localization error but ~ 10 for the distance error. Therefore the number of galaxies in the error volume is much reduced by considering the precession.

ACKNOWLEDGMENTS

T. T. is supported by International Graduate Program for Excellence in Earth-Space Science (IGPEES). A. N. is supported by JSPS KAKENHI Grant Nos. JP19H01894 and JP20H04726 and by Research Grants from Inamori Foundation. S. M. is supported by NSF PHY-1912649.

DATA AVAILABILITY

The data underlying this article will be shared on reasonable request to the corresponding author.

REFERENCES

- Aasi J., et al., 2015, *Classical and Quantum Gravity*, 32, 074001
 Abadie J., Abbott B. P., et al., 2010, *Classical and Quantum Gravity*, 27, 173001
 Abbott B. P., et al., 2016, *Living Reviews in Relativity*, 19
 Abbott B. P., et al., 2017a, *Classical and Quantum Gravity*, 34, 044001
 Abbott B., et al., 2017b, *Physical Review Letters*, 119
 Abbott B. P., et al., 2017c, *Astrophys. J.*, 848, L12
 Abbott R., Abbott T. D., et al., 2020, *The Astrophysical Journal*, 896, L44
 Abbott R., Abbott T. D., et al., 2021a, GWTC-3: Compact Binary Coalescences Observed by LIGO and Virgo During the Second Part of the Third Observing Run ([arXiv:2111.03606](https://arxiv.org/abs/2111.03606))
 Abbott R., Abbott T. D., et al., 2021b, *The Astrophysical Journal Letters*, 915, L5
 Acernese F., et al., 2015, *Classical and Quantum Gravity*, 32, 024001
 Acharyya A., Agudo I., et al., 2019, *Astroparticle Physics*, 111, 35
 Adhikari R. X., et al., 2020, *Classical and Quantum Gravity*, 37, 165003
 Apostolatos T. A., Cutler C., Sussman G. J., Thorne K. S., 1994, *Phys. Rev. D*, 49, 6274
 Baltus G., Janquart J., Lopez M., Reza A., Caudill S., Cudell J.-R., 2021, *Phys. Rev. D*, 103, 102003
 Barthelmy S. D., et al., 2005, *Space Science Reviews*, 120, 143–164
 Bartos I., et al., 2018, *Monthly Notices of the Royal Astronomical Society*, 477, 639–647
 Brown D. A., Lundgren A., O’Shaughnessy R., 2012, *Phys. Rev. D*, 86, 064020
 Cannon K., Cariou R., et al., 2012, *The Astrophysical Journal*, 748, 136
 Chan M. L., Messenger C., Heng I. S., Hendry M., 2018, *Phys. Rev. D*, 97, 123014
 Creighton J. D. E. J. D. E., Anderson W. G., 2011, Gravitational-wave physics and astronomy : an introduction to theory, experiment and data analysis. Wiley-VCH, <http://ci.nii.ac.jp/ncid/BB07081613>

- Cutler C., Flanagan E. E., 1994, *Phys. Rev. D*, 49, 2658
- Degallaix (the Virgo Collaboration) J., 2018, Advanced Virgo+ preliminary studies, <https://tds.virgo-gw.eu/?content=3&r=14287>
- Digel S., Myers J. D., 2001, GLAST: Exploring Nature’s Highest Energy Processes with the Gamma-ray Large Area Space Telescope, NASA STI/Recon Technical Report N
- Foucart F., Hinderer T., Nissanke S., 2018, *Phys. Rev. D*, 98, 081501
- Harry G. M., 2010, *Classical and Quantum Gravity*, 27, 084006
- Husa S., Khan S., Hannam M., Pürrer M., Ohme F., Forteza X. J., Bohé A., 2016, *Phys. Rev. D*, 93, 044006
- Ivezic Ž., et al., 2019, *The Astrophysical Journal*, 873, 111
- Jefremov P. I., Tsupko O. Y., Bisnovatyi-Kogan G. S., 2015, *Phys. Rev. D*, 91, 124030
- Kapadia S. J., Singh M. K., Shaikh M. A., Chatterjee D., Ajith P., 2020, *The Astrophysical Journal*, 898, L39
- Khan S., Husa S., Hannam M., Ohme F., Pürrer M., Forteza X. J., Bohé A., 2016, *Phys. Rev. D*, 93, 044007
- Lundgren A., O’Shaughnessy R., 2014, *Phys. Rev. D*, 89, 044021
- Magee R., Borhanian S., 2022, Realistic observing scenarios for the next decade of early warning detection of binary neutron stars ([arXiv:2201.11841](https://arxiv.org/abs/2201.11841))
- Magee R., Chatterjee D., et al., 2021, First Demonstration of Early Warning Gravitational-wave Alerts, [doi:10.3847/2041-8213/abed54](https://doi.org/10.3847/2041-8213/abed54), <https://doi.org/10.3847/2041-8213/abed54>
- Maggiore M., 2008, Gravitational Waves: Volume 1: Theory and Experiments. Gravitational Waves, OUP Oxford, <https://books.google.co.jp/books?id=AqVpQgAACAAJ>
- McWilliams S. T., Levin J., 2011, *The Astrophysical Journal*, 742, 90
- Metzger B. D., 2019, *Living Reviews in Relativity*, 23
- Michimura Y., Komori K., et al., 2020, *Phys. Rev. D*, 102, 022008
- Nakar E., 2007, *Physics Reports*, 442, 166
- Nishizawa A., 2016, *Phys. Rev. D*, 93, 124036
- Nishizawa A., 2017, *Phys. Rev. D*, 96, 101303
- Nitz A. H., Canton T. D., 2021, arXiv e-prints, p. arXiv:2106.15259
- Nitz A. H., Schäfer M., Canton T. D., 2020, *The Astrophysical Journal*, 902, L29
- Punturo M., et al., 2010, *Classical and Quantum Gravity*, 27, 194002
- Sachdev S., Magee R., et al., 2020, An Early-warning System for Electromagnetic Follow-up of Gravitational-wave Events, [doi:10.3847/2041-8213/abc753](https://doi.org/10.3847/2041-8213/abc753), <https://doi.org/10.3847/2041-8213/abc753>
- Schutz B., 1986, *Nature*, 323, 310
- Singh M. K., Kapadia S. J., Shaikh M. A., Chatterjee D., Ajith P., 2021, *Monthly Notices of the Royal Astronomical Society*, 502, 1612–1622
- Smith R., Field S. E., Blackburn K., Haster C.-J., Pürrer M., Raymond V., Schmidt P., 2016, *Phys. Rev. D*, 94, 044031
- Somiya K., 2012, *Classical and Quantum Gravity*, 29, 124007
- Tsang D., Read J. S., Hinderer T., Piro A. L., Bondarescu R., 2012, *Phys. Rev. Lett.*, 108, 011102
- Tsutsui T., Nishizawa A., Morisaki S., 2021, *Physical Review D*, 104
- Vecchio A., 2004, *Physical Review D*, 70
- Vitale S., Lynch R., Veitch J., Raymond V., Sturani R., 2014, *Physical Review Letters*, 112
- Wei W., Huerta E., 2021, *Physics Letters B*, 816, 136185
- Will C. M., Wiseman A. G., 1996, *Physical Review D*, 54, 4813–4848
- Yu H., Adhikari R. X., Magee R., Sachdev S., Chen Y., 2021, arXiv e-prints, p. [arXiv:2104.09438](https://arxiv.org/abs/2104.09438)

This paper has been typeset from a $\text{\TeX}/\text{\LaTeX}$ file prepared by the author.